Published in "Journal of Molecular Structure 1072: 267–276, 2014"
which should be cited to refer to this work.



# A new mixed-ligand copper(II) complex of (*E*)-*N*′-(2-hydroxybenzylidene) acetohydrazide: Synthesis, characterization, NLO behavior, DFT calculation and biological activities

S. Yousef Ebrahimipour [a,*], Iran Sheikhshoaie [a], Aurelien Crochet [b], Moj Khaleghi [c], Katharina M. Fromm [d]

[a] *Department of Chemistry, Shahid Bahonar University of Kerman, 7616914111, Kerman, Iran*
[b] *FriMat, University of Fribourg, Chemin du Musée 6, CH-1700 Fribourg, Switzerland*
[c] *Department of Biology, Shahid Bahonar University of Kerman, 7616914111, Kerman, Iran*
[d] *Department of Chemistry, University of Fribourg, Chemin du Musée 9, CH-1700 Fribourg, Switzerland*

## HIGHLIGHTS

- Crystal structure of a new mixed ligand Cu(II) complex has been determined by single crystal X-ray diffraction analysis.
- The electronic nature of the compounds have been investigated *via* DFT calculations.
- NBO, vibrational and UV-Vis spectral analysis were carried out.
- The antimicrobial activities of compounds were evaluated against microorganisms.

## GRAPHICAL ABSTRACT

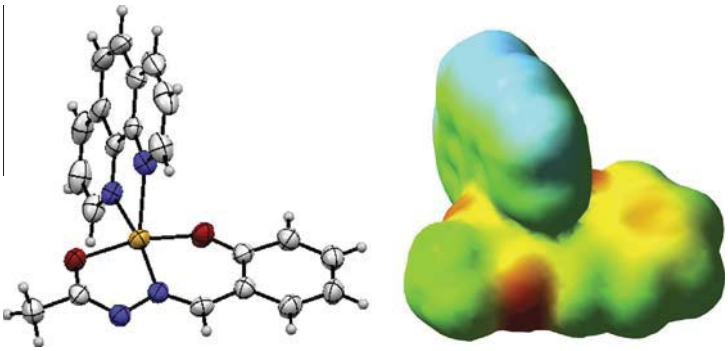

A tridentate hydrazone Schiff base ligand, (*E*)-*N*′-(2-hydroxybenzylidene)acetohydrazide [HL], and its mixed-ligand Cu(II) complex [CuL(phen)], have been synthesized and characterized by elemental analyses, FT-IR, molar conductivity, UV–Vis spectroscopy. The structure of the complex has been determined by X-ray diffraction. This complex has square pyramidal geometry and the positions around central atom are occupied with donor atoms of Schiff base ligand and two nitrogens of 1,10-phenanthroline. Computational studies of compounds were performed by using DFT calculations. The linear polarizabilities and first hyperpolarizabilities of the studied molecules indicate that these compounds can be good candidates of nonlinear optical materials. It is in accordance with experimental data. In addition, *invitro* antimicrobial results show that these compounds specially [CuL(phen)] have great potential of antibacterial activity against *Escherichia coli, Staphylococcus aureus, Pseudomonas aeruginosa, Listeria monocytogenes* bacteria and antifungal activity against *Candida Albicans* in comparison to some standard drugs.

## Introduction

Nowadays, copper(II) Schiff base complexes have attracted great attention in coordination chemistry due to their different applications [1,2]. Copper(II) complexes can act as efficient catalysts in many chemical processes. Also many reports have shown that they are suitable candidates for NLO materials [3,4].

* Corresponding author. Tel./fax: +98 (341) 3222033.
*E-mail addresses:* ebrahimipour@uk.ac.ir, ebrahimipour@ymail.com (S. Yousef Ebrahimipour).

In bioinorganic chemistry, major interest of researches on Cu(II) complexes have been focused on their similarity of structures to metaloproteins and providing models for the metal-containing sites in these proteins and enzymes such as superoxide dismutases [5,6]. This metalloenzyme plays a key role in the protection of cell against potentially toxic derivatives of biological activated oxygen. Superoxide dismutases carry one copper and one adjacent ion in active catalytic center [7–9].

Also heterocyclic ligands like 1,10-phenanthroline and their complexes have been in concentration due to their wide range of biological properties such as DNA binding, anti-microbial, anti-cancer and antioxidant activities [10–13]. There are few report of mixed ligand Cu(II) complexes with hydrazone ONO Schiff base and 1,10-phenanthroline [14] therefore investigation of properties of this class of compounds can be useful for development of applications of them in different areas.

In our previous work we discussed that biochemical activity of mixed ligand complexes of Cu(II) complex with $CuL_1L_2$ formula depends on non-covalent interaction between aromatic units [15].

Based upon, hydrazone derivative compound, (*E*)-*N*′-(2-hydroxybenzylidene)acetohydrazide [HL], and its mixed ligand Cu(II) complex were prepared and characterized by various physicochemical methods. DFT calculations have been performed to investigate detailed experimental spectroscopic data and NLO properties of synthesized compounds. Also, the biological activities of the mentioned compounds as antimicrobial agents especially against Gram-positive and Gram-negative bacteria were investigated.

## Experimental

### *Materials and instrumentation*

All chemicals were analytical grade and were used as received. Elemental analyses of C, H and N were performed on a Heracuse CHN rapid analyzer. The FT-IR spectrum was recorded on a Nicolet-Impact 400D spectrometer (4000–400 $cm^{-1}$) in KBr pellets. Conductance measurements were made by means of a Metrohm 712 Conductometer in DMSO. $^1$H NMR spectrum was recorded at 25 °C with a Bruker BRX 100 AVANCE spectrometer. The electronic spectra were recorded in DMSO on a Cary 50 UV–Vis spectrophotometer. Melting point was determined on a Gallenkamp melting point apparatus. Crystal was mounted on loop and all geometric and intensity data were taken from a single crystal. Data collection using Mo *K*α radiation ($\lambda$ = 0.71073 Å) was performed at 200 K with a Stoe IPDS II diffractometer, equipped with an oxford cryostat. The SHG efficiency of [CuL(phen)] was measured with respect to urea by the powder technique developed by Kurtz and Perry using a Q switched Nd-YAG laser (1064 nm, 10 ns, 10 Hz). The homogeneous powder was mounted in the path of a laser beam of pulse energy 2.2 mJ obtained by the split beam technique.

### *Synthesis of (E)-N′-(2-hydroxybenzylidene)acetohydrazide [HL]*

In typical procedure [16], an ethanolic solution (4 ml) of 2-hydroxybenzaldehyde (0.025 g, 0.2 mmol) was added to 3 ml ethanolic solution of acetohydrazide (0.015 g, 0.2 mmol). The mixture was stirred for 10 min. the resulting white precipitate was separated by filtration, washed with cold ethanol and dried in a desiccator over anhydrous $CaCl_2$.

Yield: 0.028 g, 78%. m.p.: 199 °C. Anal. Calc. for $C_{10}H_{11}N_2O_2$ (178.19 g $mol^{-1}$): C, 60.66; H, 5.66; N, 15.72. Found: C, 60.14; H, 5.43; N, 15.78%. FT-IR (KBr), $cm^{-1}$: $\nu$(OH) 3186, $\nu$(N—H) 3074, $\nu$(C═H)$_{aro}$ 2869–2947, $\nu$(C═O) 1678, $\nu$(C═N) 1616, $\nu$(C═C$_{ring}$) 1489, $\nu$(C—O) 1315, $\nu$(N—N) 1114. $^1$H NMR (100 MHz, DMSO-$d_6$, 25 °C, ppm): $\delta$ = 11.7 (s, 1H; O$^1$H), 10.9 (s, 1H; N$^4$H), 8.1 (s, 1H; C$^7$), 6.8–7.7 (m, 4H; C5), 2.1 (s, 3H; $C_1$, $C_3$). UV/Vis (DMSO), $\lambda_{max}$, nm ($\varepsilon$, L $mol^{-1}$ $cm^{-1}$): 284(39,558), 293(36,306), 326(27,715).

### *Preparation of (1,10-phenanthroline)[(E)-N′-(2-hydroxybenzylidene) acetohydrazide] copper(II) [CuL(phen)]*

$Cu(OAc)_2{\cdot}4H_2O$ (0.1 mmol, 0.02 g) was added to a solution of [HL] (0.1 mmol, 0.018 g) and NaOH (0.2 mmol, 0.01 g) in 5 mL of boiling ethanol and the mixture was refluxed in a water bath for 10 min. 1,10-Phenanthroline (0.1 mmol, 0.02 g) was added to the resulting dark-green colored solution which was further refluxed for *ca.* 1 h. After cooling, the precipitate was separated and then recrystallized from dichloromethane–methanol to give green single crystal and were dried in a vacuum desiccator over $CaCl_2$.

Yield: 0.030 g, 72%. m.p.:>300 °C. Molar conductance ($10^{-3}$ M, DMSO) 17.0 $ohm^{-1}$ $cm^2$ $mol^{-1}$. Anal. Calc. for $C_{21}H_{16}CuN_4O_2$ (419.92 g $mol^{-1}$): C, 60.06; H, 3.84; N, 13.34. Found: C, 60.17; H, 3.71; N, 13.45%. FT-IR (KBr), $cm^{-1}$: $\nu$(C═N) 1612, $\nu$(C═C$_{ring}$) 1512, $\nu$(C—O) 1303, $\nu$(N—N) 1103. UV/Vis (DMSO, $\lambda_{max}$, nm ($\varepsilon$, L $mol^{-1}$ $cm^{-1}$): 282(35,901), 319(17,097), 389(10,138), 652(192).

### *Computational methods*

The geometry of the synthesized compounds was fully optimized without any symmetry constraints using density functional theory (DFT), B3LYP exchange correlation functional and 6-31+G(d,p) [17,18] with Gaussian 03 program package [19]. X-ray Crystal structure used as starting point for Calculations. The optimized structures were characterized by frequency calculations as true minima. The density functional theory has been used to calculate the dipole moment ($\mu$), mean polarizability ($\alpha$) and the total first static hyperpolarizability ($\beta$) for [HL] and [CuL(phen)] in terms of *x*, *y*, *z* components and are given by following equations [20].

$$\mu = \left(\mu_x^2 + \mu_y^2 + \mu_z^2\right)^{1/2}$$

$$\alpha = \frac{1}{3}(\alpha_{xx} + \alpha_{yy} + \alpha_{zz})$$

$$\beta_{tot} = [(\beta_{xxx} + \beta_{xyy} + \beta_{xzz})^2 + (\beta_{yyy} + \beta_{yzz} + \beta_{yxx})^2 + (\beta_{zzz} + \beta_{zyy} + \beta_{zxx})^2]^{1/2}$$

The polarizability and hyperpolarizability tensors ($\alpha_{xx}$, $\alpha_{xy}$, $\alpha_{yy}$, $\alpha_{xz}$, $\alpha_{yz}$, $\alpha_{zz}$ and $\beta_{xxx}$, $\beta_{xxy}$, $\beta_{xyy}$, $\beta_{yyy}$, $\beta_{xxz}$, $\beta_{xyz}$, $\beta_{yyz}$,$\beta_{xzz}$, $\beta_{yzz}$, $\beta_{zzz}$) can be obtained by a frequency job output file of Gaussian. However, $\alpha$ and $\beta$ values of Gaussian output are in atomic units (a.u.) so they have been converted into electrostatic units (esu) ($\alpha$; 1 a.u. = $0.1482 \times 10^{-24}$ esu, $\beta$; 1 a.u. = $8.6393 \times 10^{-33}$ esu). Furthermore, determination of the origin of structural behaviors had been done with Natural Band Orbital (NBO) and Wiber index analysis (WBI) at the same level [21]. UV–Vis spectra, electronic transitions, absorbance and oscillator strengths were computed with the time-dependent DFT (TD-DFT) method at the B3LYP/6-31+G(d,p) level. Solvent (DMSO) was considered as a uniform dielectric constant 46.7 and Polarized Continuum Model (PCM). GAUSSSUM 3.0 with FWHM 0.3 eV have been used for analyzing the contribution percentage of groups and atoms to the molecular orbitals [22].

### *Crystal structure determination*

Absorption correction was partially integrated in the data reduction procedure [23]. The structure was solved refined using full-matrix least-squares on $F^2$ with the SHELX-97 package [24].

**Table 1**
Crystal data and structure refinement for [CuL(phen)].

| | | |
|---|---|---|
| Empirical formula | $C_{21}$ $H_{16}$ Cu $N_4$ $O_2$ | |
| Formula weight | 419.92 | |
| Temperature | 200(2) K | |
| Wavelength | 0.71073 Å | |
| Crystal system | Monoclinic | |
| Space group | $P\,2_1/c$ | |
| Unit cell dimensions | $a$ = 10.9518(5) Å | $\alpha$ = 90° |
| | $b$ = 11.7188(7) Å | $\beta$ = 96.856(4)° |
| | $c$ = 13.7990(7) Å | $\gamma$ = 90° |
| Volume | 1758.33(16) Å3 | |
| Z | 4 | |
| Density (calculated) | 1.586 Mg/m3 | |
| Absorption coefficient | 1.268 $mm^{-1}$ | |
| $F(000)$ | 860 | |
| Crystal size | 0.240 × 0.143 × 0.080 mm3 | |
| Theta range for data collection | 1.87–25.00° | |
| Index ranges | $-13 \leqslant h \leqslant 13$, | |
| | $-13 \leqslant k \leqslant 13$, $-16 \leqslant l \leqslant 16$ | |
| Reflections collected | 21,995 | |
| Independent reflections | 3096 [$R$(int) = 0.0448] | |
| Completeness to theta = 25.00° | 100.0% | |
| Absorption correction | Integration | |
| Max. and min. transmission | 0.8329 and 0.6782 | |
| Refinement method | Full-matrix least-squares on $F2$ | |
| Data/restraints/parameters | 3096/0/254 | |
| Goodness-of-fit on $F2$ | 0.973 | |
| Final $R$ indices [$I$ > 2sigma(I)] | $R1$ = 0.0297, w$R2$ = 0.0745 | |
| $R$ indices (all data) | $R1$ = 0.0447, w$R2$ = 0.0786 | |
| Largest diff. peak and hole | 0.240 and −0.384 e.Å$^{-3}$ | |

A summary of the crystal data and refinement details for the [CuL(phen)] are given in Table 1.

*Determination of antimicrobial activity*

The four bacterial strains and *Candida albicans* used in the present study were the clinical isolates obtained from Afzalipour Hospital in Kerman, Iran. The used bacteria were *Escherichia coli, Staphylococcus aureus, Pseudomonas aeruginosa,* and *Listeria monocytogenes*. The antimicrobial effect of [HL] and [CuL(phen)] on the microorganisms were assayed by Agar well diffusion method [25]. Mueller–Hinton medium (Merck) for bacteria and YGC medium (Merck) for yeast strain was used as the test medium. Also, the minimum concentrations of the compounds to inhibit the microorganisms (MIC) were determined by the micro broth dilutions technique strictly following the National Committee for Clinical Laboratory Standards (NCCLS) recommendations [26]. The inoculum was prepared using a 4–6 h broth culture of each bacteria and 24 culture of yeast strains adjusted to a turbidity equivalent to a 0.5 McFarland standard [27]. Petriplates containing 20 ml Agar test plates were seeded with 24 h culture of microorganism strains. Wells were cut and 100 μl of the compounds (5000 μg/ml; DMSO was used as solvent) were added. The plates were then incubated at 37 °C for 24 h. The antibacterial activity was assayed by measuring the diameter of the inhibition zone formed around the well. DMSO as solvent was used as a negative control whereas media with ciprofloxacin (standard antibiotic) and fluconazole (standard antifungal drug) were used as the positive controls. The experiments were performed in triplicate. Serial dilutions ranging from 5000 μg/mL to 4.9 μg/mL were prepared in medium.

## Results and discussion

The [HL] ligand (Scheme 1) can exist in two main tautomeric forms. Spectroscopic analysis shows that *enolic* form is preferred in complexation with $Cu(OAc)_2.4H_2O$. [HL] and [CuL(phen)] are stable in air and soluble in most solvents except water and *n*-hexane. Molar conductivity values of Cu(II) complex equal to 17 $ohm^{-1}$ $cm^2$ $mol^{-1}$ in DMSO, indicating non-electrolyte behaviors of it.

*X-ray crystal structure*

An ORTEP view of Cu is presented in Fig. 1. Also a unit cell of [CuL(phen)] by 50% thermal ellipsoid is shown in Fig. 2. Selected bond distance and interatomic angles are listed in Table 2. In this structure Cu(II) has a five coordination sphere in which central atom is surrounded by donor atoms of tridentate ONO Schiff base and two nitrogen atoms from bidentate heterocyclic ligand. X-ray analysis data shows that Cu complex has a distorted square pyramidal with trigonality index of 5% that square plane is made up of donor atoms of [HL] and one nitrogen atom of 1,10-phenanthro-

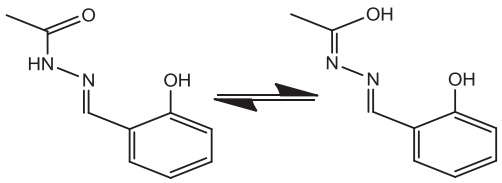


**Scheme 1.** The main tautomeric forms of the free ligand [HL].

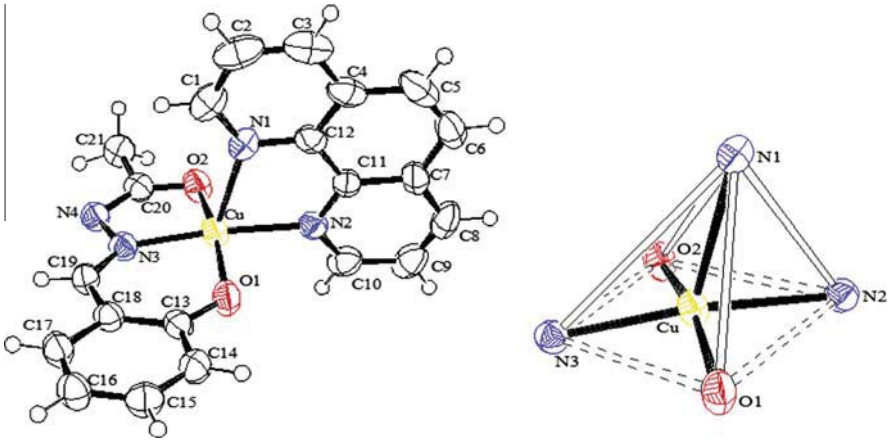


**Fig. 1.** Perspective view of complex with displacement ellipsoids drawn at the 50% level.

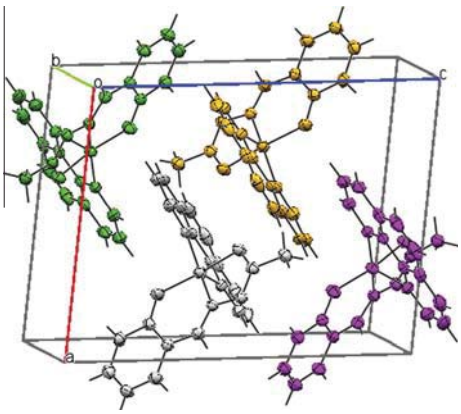

**Fig. 2.** ORTEP drawing of unit cell of the complex [CuL(phen)].

**Table 2**
Selected calculated and experimental bond lengths (Å) and bond angles (°) for [CuL(phen)].

| Type | Exp | Calc. | Type | Exp | Calc. |
|---|---|---|---|---|---|
| Cu1—N3 | 1.935(2) | 1.947 | N3—Cu1—O1 | 93.01(8) | 93.9 |
| Cu1—O1 | 1.919(2) | 1.912 | N3—Cu1—N2 | 168.91(8) | 170.3 |
| Cu1—N2 | 2.049(2) | 2.108 | N3—Cu1—O2 | 80.21(8) | 80.9 |
| Cu1—O2 | 1.949(2) | 1.964 | N3—Cu1—N1 | 113.86(8) | 112.9 |
| Cu1—N1 | 2.309(2) | 2.411 | O1—Cu1—N2 | 90.20(8) | 91.1 |
| N3—N4 | 1.404(3) | 1.385 | O1—Cu1—O2 | 165.92(8) | 168.7 |
| N3—C19 | 1.280(3) | 1.296 | N2—Cu1—O2 | 94.29(8) | 92.6 |
| O1—C13 | 1.308(3) | 1.309 | N2—Cu1—N1 | 76.50(8) | 74.3 |
| O2—C20 | 1.282(3) | 1.298 | Cu1—N3—N4 | 115.3(1) | 114.9 |
| C13—C18 | 1.417(3) | 1.439 | Cu1—N3—C19 | 126.7(2) | 126.2 |
| N4—C20 | 1.306(3) | 1.318 | N4—N3—C19 | 117.9(2) | 118.9 |
| C19—C18 | 1.440(4) | 1.439 | Cu1—O1—C13 | 125.7(2) | 126.6 |
| | | | Cu1—O2—C20 | 110.9(2) | 109.5 |
| | | | O1—C13—C18 | 124.3(2) | 124.7 |
| | | | N3—N4—C20 | 108.2(2) | 109.3 |
| | | | N3—C19—C18 | 124.0(2) | 124.8 |
| | | | O2—C20—N4 | 125.2(2) | 125.2 |

line, also another nitrogen of heterocyclic ligand occupies the axial position.

Trigonality indexed is defined by $\beta-\alpha/60$ that beta and alpha are the two largest bond angles around the metal center in five coordinated environment. An ideal square pyramid have $\beta = 180°$ and $\alpha = 180°$ and therefore $\tau = 0\%$, but an ideal trigonal-bipyramidal structure will have $\beta = 180°$ and $\alpha = 120°$ and $\tau$ is equal to 100% [28].

As can be seen in packing diagram (Fig. 3) there are pi–pi interaction in lattice which stabilize crystal structure of compound.

These interactions occurs between two 1,10-phenanthroline of neighbors molecules, the distances are reported in Table 3. The two central centroid, Cg(6), are distant of 3.6119(16) Å with a perpendicular distance of 3.4144(11) Å and a slippage of 1.178 Å. The overlap of phenanthroline ligand is, for the best of our knowledge, the most important for this type of compound (copper phenanthroline and 2-hydroxybenzylidene) hydrazide type [29–31].

*Geometry optimization*

The geometry of the compounds was optimized using DFT method with the B3LYP function. In order to get more stable structure for the ligand, all the proposed tautomers were optimized at B3LYP/6-31+G(d,p) level of theory and result is shown in Fig. 4. According to this, ***a*** owns a more stable structure that is accordance with X-ray data of ligand, so that we performed other calculations on the basis of ***a***.

Geometrical calculated parameters are listed in Table 2. According to it, there is a good agreement between structural parameters from DFT calculation and X-ray crystallography result. Maximum deviations are 0.102 Å and 2.7° for the Cu1-N1 bond and the O1—Cu1—O2 angle, respectively. A little difference between theoretical and experimental values may origin from this fact that the experimental data was obtained in the solid state, while the calculated values are concerned to single molecules in the gaseous state without considering lattice interactions.

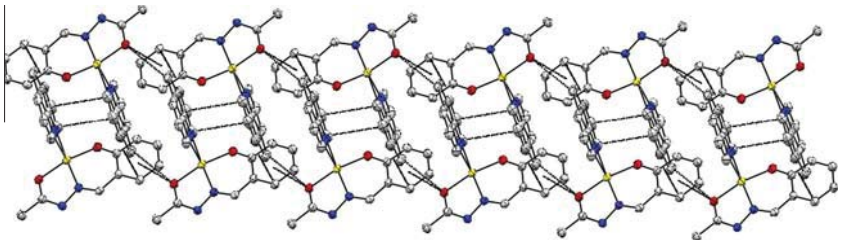

**Fig. 3.** Illustration of $\pi$-stacking interaction in [CuL(phen)] with hydrogen omitted for clarity.

**Table 3**
Analysis of short ring-interactions with Cg–Cg distances.

| Cg(i) | Cg(j) | Cg(i)–Cg(j) (Å) | Cg(i)–Perp(j) (Å) | Cg(j)–Perp(i) (Å) | Slippage (Å) |
|---|---|---|---|---|---|
| Cg(4) | Cg(4) | 4.7612(17) | 3.1262(11) | 3.1262(11) | 3.591 |
| | Cg(5) | 3.8553(16) | 3.3877(11) | 3.4340(11) | |
| | Cg(6) | 4.5046(17) | 3.3748(11) | 3.4422(11) | |
| Cg(5) | Cg(4) | 3.8554(16) | 3.4340(11) | 3.3878(11) | 3.609 |
| | Cg(5) | 4.9900(15) | 3.4460(11) | 3.4460(11) | |
| | Cg(6) | 3.6315(15) | 3.4028(11) | 3.4191(11) | |
| Cg(6) | Cg(4) | 4.5047(17) | 3.4422(11) | 3.3749(11) | 1.178 |
| | Cg(5) | 3.6316(15) | 3.4192(11) | 3.4028(11) | |
| | Cg(6) | 3.6119(16) | 3.4144(11) | 3.4143(11) | |

Cg(4): C1 C2 C3 C4 C12 N1; Cg(5): C7 C8 C9 C10 N2 C11; Cg(6): C4 C5 C6 C7 C11 C12; Cg(i)–Cg(j): Distance between ring Centroids (Å); Cg(i)–Perp(j): Perpendicular distance of Cg(i) on ring j (Å); Cg(j)–Perp(i): Perpendicular distance of Cg(j) on ring i (Å); Slippage: Distance between Cg(i) and Perpendicular Projection of Cg(j) on ring i (Å).

*Vibrational analysis*

Assignments of selected prominent IR bands in the 400–4000 $cm^{-1}$ region for [HL] and its Cu(II) complex are listed in the Experimental section. The observed and calculated FT-IR spectra of [CuL(phen)] are also shown in Fig. 5. For more investigation, selected experimental and scaled calculated vibrational frequencies of title complex are compared in Table 4. In the FT-IR

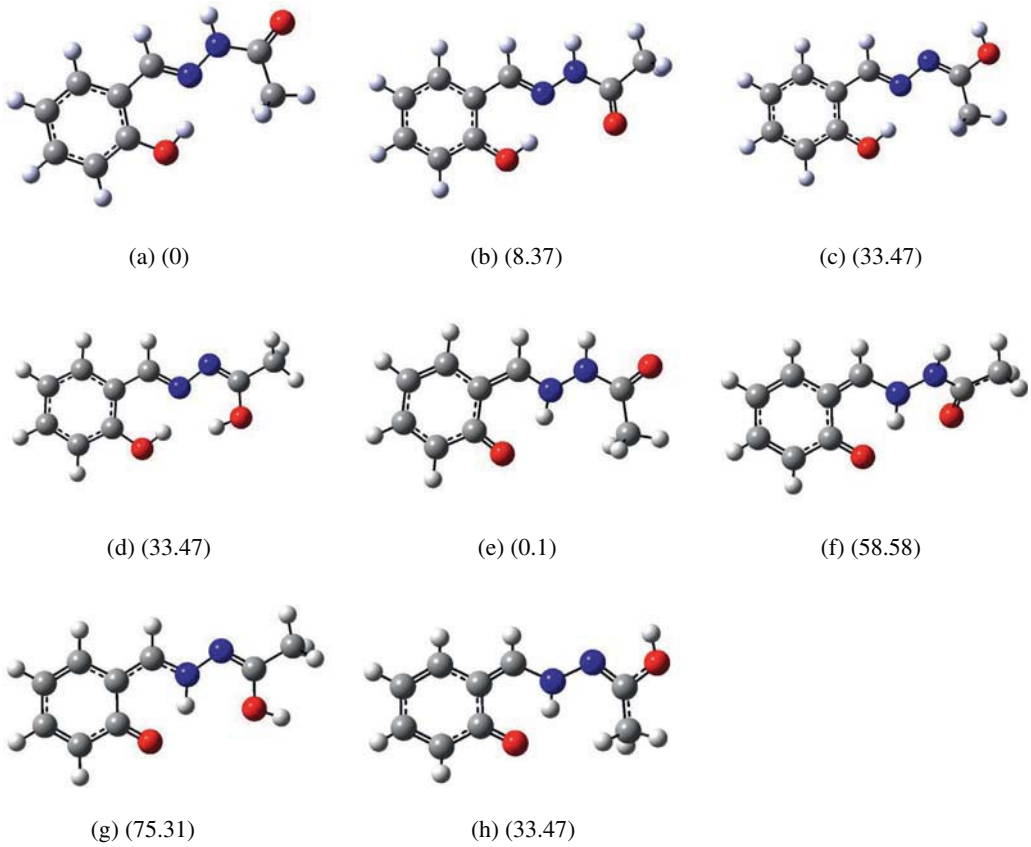

(a) (0) (b) (8.37) (c) (33.47)

(d) (33.47) (e) (0.1) (f) (58.58)

(g) (75.31) (h) (33.47)

**Fig. 4.** The optimized geometries of the possible tautomeric forms of [HL].

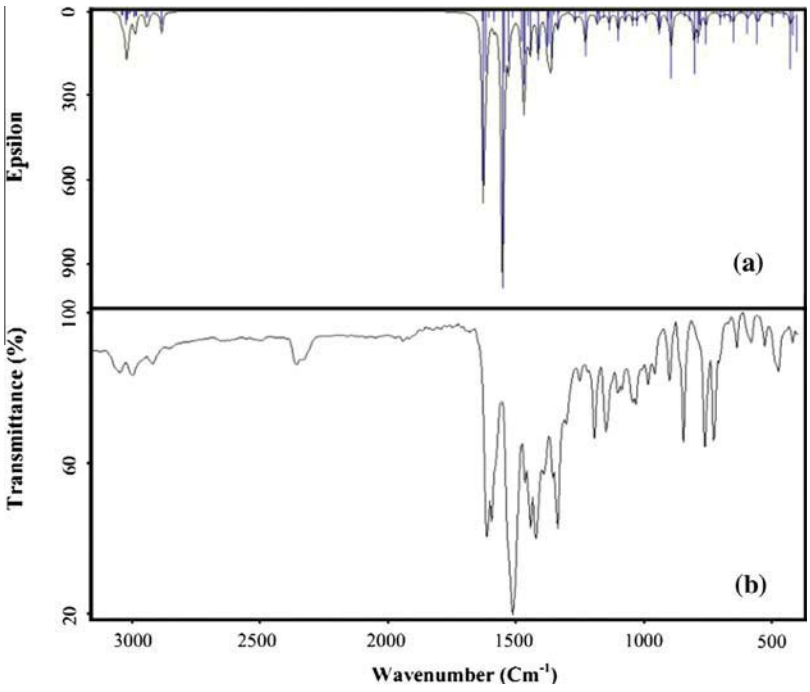


**Fig. 5.** Calculated (a) and Experimental (b) FT-IR spectra of [CuL(phen)].

**Table 4**
Vibrational assignments of FT-IR peak along with the theoretically computed wavenumber.

| Experimental | Calculated B3LYP/6-31+G(d,p) | | Assignment |
|---|---|---|---|
| FT-IR, $cm^{-1}$ | Unscaled | Scaled* | |
| 3124.90 | 3224.23 | 3104.933 | $\nu$CH II |
| 3050.83 | 3171.44 | 3054.097 | $\nu$CH I |
| 3004.03 | 3119.01 | 3003.597 | $\nu$CH $_{azm}$ |
| 3000.68 | 3110.08 | 2995.007 | $\nu_{asy}$ $CH_3$ |
| 2922.44 | 3051.05 | 2938.161 | $\nu_{sy}$ $CH_3$ |
| 1612.41 | 1668.83 | 1607.083 | $\nu$CN $_{azm}$ |
| 1596.83 | 1659.98 | 1598.561 | $\nu$CN II, $\nu$CC II |
| 1512.14 | 1578.96 | 1520.538 | $\nu$CC I |
| 1445.53 | 1494.23 | 1438.943 | $\nu$CC I, $\nu$ $C_{18}C_{19}$ |
| 1423.56 | 1489.53 | 1434.417 | $\sigma CH_{3\ asy}$ |
| 1338.86 | 1399.88 | 1348.084 | $\delta_{sy}$ $CH_3$, $\delta$ $C_{19}H$ |
| 1321.23 | 1376.89 | 1325.945 | $\nu C_{20}O_2$ |
| 1303.81 | 1347.55 | 1297.691 | $\nu$CO I |
| 1252.67 | 1297.45 | 1249.444 | $\delta_{ipb}$ CH II |
| 1195.34 | 1243.49 | 1197.481 | $\delta_{ipb}$ CH I |
| 1103.21 | 1152.86 | 1110.204 | $\nu$NN |
| 759.90 | 781.42 | 752.5075 | $\delta$ $_{opb}$ CH II |
| 729.83 | 761.2 | 733.0356 | $\delta_{opb}$ CH I |
| 582.81 | 607.72 | 585.2344 | $\nu$CuO |
| 475.35 | 490.22 | 472.0819 | $\nu$CuN |

*Abbreviation:* $\nu$; stretching, $\delta$; bending, asy; asymmetric, sy; symmetric, ipb; in plane bending, opb; out of plane bending, I; aldehyde ring, II; 1,10-phenanthroline rings, azm; azomethine.

spectrum of the ligand, a sharp band with high intensity at 1678 $cm^{-1}$ is assigned to C═O vibrations [32]. The OH and NH vibrations are located at 3186 and 3074 $cm^{-1}$ respectively [33]. The absence of these frequencies and the red shift of the C—O band from (1315 $cm^{-1}$) to (1303 $cm^{-1}$) in [CuL(phen)] indicate ligand in the *enolic* form coordinates to the metal center through deprotonated phenolic and aliphatic oxygen atoms [34]. This band is observed at 1297.7 $cm^{-1}$ in the calculation.

Also in the [HL], strong band at 1616 $cm^{-1}$ is assigned to vibrations of the azomethine moiety while on complexation, it appearing at 1612 $cm^{-1}$ shows that the azomethine nitrogen atom of ligand coordinates to central atom [15], the DFT calculation gives this band at 1607 $cm^{-1}$.

### *Molecular electrostatic potential*

Molecular electrostatic potential (MEP) is used for identifying chemical reactivities as well as presence of intra and intermolecular interactions on the skeleton of compound [35]. Molecular electrostatic potential of ligand and complex is shown in Fig. 6. In these figures, different colors are used to distinguish different values of electronic potential. The red colors are correlated with electron rich area while the blue is used for representation of electronpositive sites. According to Fig. 6 oxygens are electron rich area and suitable for nucleophilic attacks while in complex, this tendency of oxygen donor atoms have been decreased. In contrast, the configuration of the ligand while connecting to the central atom in complexation makes electrostatic potential of nitrogen shift to more negative values.

### *Frontier molecular orbitals*

Frontier molecular orbitals, i.e. the highest occupied molecular orbital (HOMO) and lowest unoccupied molecular orbital (LUMO) play an important role in the electric properties as well as, UV–Vis spectra and determination of chemical reactivity [36]. Figs. S1 and 7 shows the molecular energies orbitals with isodensity surface plots of HOMO and LUMO for [HL] and [CuL(phen)] respectively. As can be seen, The electron population of HOMO and LUMO are localized on the whole skeleton of [HL] while In [CuL(phen)], the electron density of HOMO is mainly located on the deprotonated Schiff base ligand and LUMO electron density is localized on the aromatic rings of heterocyclic moiety. Details of the frontier molecular orbitals in the complex are presented in Tables S1 and S2. HOMO–LUMO energy gap correlates with the stability of compounds. Results show that the band gaps between HOMO and LUMO equal 4.33 and 2.4 eV for [HL] and [CuL(phen)] respectively Hence, Cu(II) complex has more chemical activity than parent tridentate ligand [HL].

### *Electronic spectra*

In the electronic spectrum of [HL], three bands at 284 nm, 293 nm and 326 nm have been observed in the ligand. They can be attributed to $\pi \rightarrow \pi^*$ transitions of the phenyl ring and $\pi \rightarrow \pi^*$ and $n \rightarrow \pi^*$ of the azomethine moiety and carbonyl group respectively. The spectra of the Cu(II) complex (Fig. 8) has similar features [37,38]. The band at approximately 389 nm reveals coordination of the ligand to metal center. The high epsilon value of log $\varepsilon = 4.01$ confirms that this band is due to MLCT (metal to ligand) and LMCT (ligand to metal) charge transfer transitions. In five coordinated Cu(II) complexes Visible spectrum can be used for predicting preferred geometry. SP or distorted SP geometries exhibit a band in the 550–660 nm range that is assigned to $d_{xz}, d_{yz} \rightarrow d_{x^2-y^2}$ while TBP structures have a characteristic band around >800 nm is related to $d_{xz}, d_{x^2-y^2} \rightarrow d_{z^2}$. Spectrum of [CuL(phen)] shows a band at 652 nm, Thus Cu central atom in this complex is closer to SP [39].

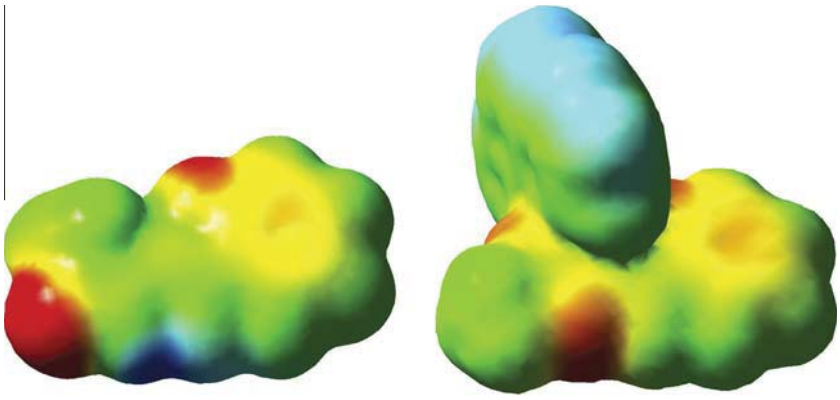

**Fig. 6.** Molecular electrostatic potential map of [HL] (left) and [CuL(phen)](right).

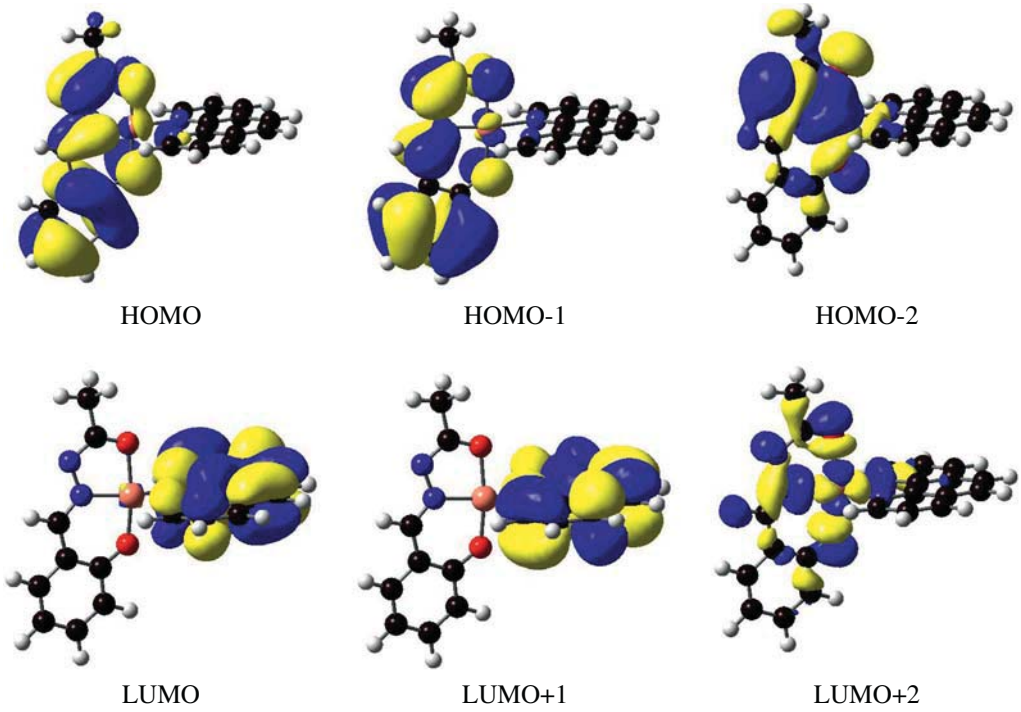


**Fig. 7.** Contour plots of some selected MOs ($\beta$-spin) of [CuL(phen)].

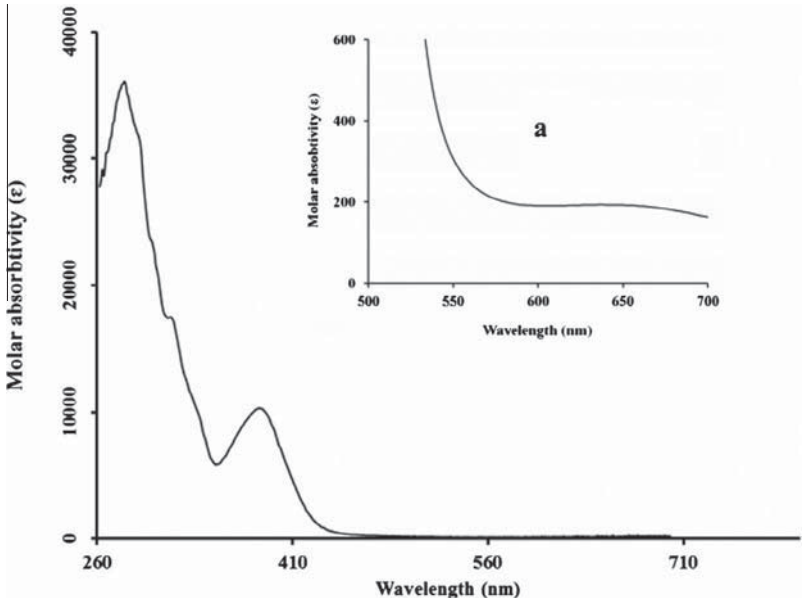


**Fig. 8.** Experimental absorption spectra of Cu(II) complex in DMSO. The *d–d* transition is shown in inset for title complex (a).

To investigate the electronic transition corresponding to these bands, TDDFT calculations have been performed at 6-31G+(d,p) level in DMSO. Summary of the results is gathered in Table 5. According to it, low energy weak transitions belonged to *d-d* transitions. Other intense bands attributed to ILCT, LMCT and MLCT. For investigation of photostability of [CuL(phen)], UV–Vis spectrum of the complex after irradiation (3 h) is shown in Fig. S3. According to it, main characteristic bands of this compound are not shifted upon irradiation of light (Xe lamp-70 W) and only small changes in band intensity was appeared.

*Natural bond orbital analysis*

NBO results show that electronic configuration of Cu(II) in complex is [core]$4S^{0.37}3d^{9.35}4p^{0.41}4d^{0.01}5p^{0.01}$. This arrangement contains 18 core electrons, 10.13 valance electrons and 0.03 rydberg electrons. These amount is consistent with calculated charge (0.8496) of Cu(II) central ion and also all coordination sites in ligands have a calculated atomic charge and electron configuration lower than expected these observations confirm significant electron donation from the donor atoms to the center metal ion. The

**Table 5**
Main calculated optical transition with composition in terms of molecular orbital contribution of the transition, vertical excitation energies and oscillator strength for [CuL(phen)].

| Composition | Weight (%) | $E$ (eV) | Oscillatory strength ($f$) | $\lambda_{max}$ (Calc.) | $\lambda_{max}$ (Exp) | Assignment |
|---|---|---|---|---|---|---|
| H-6($\beta$)– > L + 2($\beta$) | 76 | 1.5072 | 0.0008 | (675.82) | 652(2.32) | *d–d* |
| H-8($\beta$)– > L + 2($\beta$) | 14 | | | | | |
| H-9($\beta$)– > L($\beta$) | 44 | 1.9609 | 0.0005 | 442.596 | | MLCT, ILCT |
| H-1($\beta$)– > L($\beta$) | 25 | | | | | |
| H-10($\beta$)– > L($\beta$) | 48 | 2.1560 | 0.0004 | 402.542 | | MLCT |
| H-16 ($\beta$)– > L + 2($\beta$) | 53 | 2.2899 | 0.0038 | 379.015 | 389(4.01) | LMCT, MLCT |
| H-14($\beta$)– > L + 2($\beta$) | 27 | | | | | |
| H($\beta$)– > L + 3($\beta$) | 67 | 2.4330 | 0.0000 | 356.713 | | ILCT |
| H-7($\beta$)– > L($\beta$) | 29 | 2.5620 | 0.0003 | 338.758 | | ILCT |
| H($\beta$)– > L($\beta$) | 36 | | | | | |
| H($\beta$)– > L + 1($\beta$) | 19 | | | | | |
| H($\beta$)– > L + 1($\beta$) | 95 | 2.5825 | 0.0001 | 336.063 | | ILCT |
| H($\alpha$)– > L + 3($\alpha$) | 98 | 2.6317 | 0.0031 | 329.784 | 319(4.23) | ILCT |
| H($\beta$)– > L + 1($\beta$) | 16 | 2.7569 | 0.0006 | 314.804 | | ILCT |
| H($\beta$)– > L + 3($\beta$) | 77 | | | | | |
| H($\alpha$)>L + 3($\alpha$) | 98 | 2.8211 | 0.0018 | 307.643 | 282(4.56) | ILCT |

**Table 6**
Charges and electron configurations for [CuL(phen)].

| Atom | Charge | Electron configuration |
|---|---|---|
| Cu | 0.84960 | [core]4S(0.37)3d(9.35)4p(0.41)4d(0.01)5p(0.01) |
| N3 | −0.34040 | [core]2S(1.31)2p(4.00)3S(0.01)3p(0.02)3d(0.01) |
| O1 | −0.69636 | [core]2S(1.65)2p(5.03)3p(0.01) |
| N1 | −0.44266 | [core]2S(1.31)2p(4.11)3p(0.02) |
| O2 | −0.71056 | [core]2S(1.68)2p(5.02)3p(0.01) |
| N2 | −0.42597 | [core]2S(1.33)2p(4.08)3p(0.01)3d(0.01) |

calculated atomic charges from the natural population analysis (NPA) are summarized in Table 6.

*Thermodynamic properties*

Title complex was studied for the purpose of the standard thermodynamic functions ;enthalpy ($H_m^0$), entropy ($S_m^0$), and capacity ($C_{p,m}^0$) at different temperatures, used by B3LYP/6-31+G(d,p) level of theory, and the details shown in Table 7 are based on this study. Its concluded from the table that, these thermodynamic values are increased with the increase of temperature from 200 K to 800 K. The fact of increasing vibrational intensities with the temperature can be the explanation for this phenomenon.

$$H_m^\circ = 1 \times 10^{-4}T^2 + 0.0347T + 203.74 (R^2 = 0.9998)$$

$$C_{p,m}^\circ - 2 \times 10^{-4}T^2 + 0.3837T - 7.1356 (R^2 = 0.9999)$$

$$S_m^\circ = -8 \times 10^{-5}T^2 + 0.3591T + 66.3 (R^2 = 1)$$

**Table 7**
Thermodynamic properties of [CuL(phen)] at different temperatures.

| Temperature (K) | Enthalpy (Kcal mol$^{-1}$) | Heat capacity (cal mol$^{-1}$ K$^{-1}$) | Entropy (cal mol$^{-1}$ K$^{-1}$) |
|---|---|---|---|
| 200 | 215.18 | 62.69 | 135.233 |
| 298.15 | 222.7 | 90.528 | 166.251 |
| 300 | 222.868 | 91.044 | 166.825 |
| 400 | 233.319 | 117.373 | 197.28 |
| 500 | 246.199 | 139.466 | 226.373 |
| 600 | 261.067 | 157.221 | 253.793 |
| 700 | 277.525 | 171.429 | 279.442 |
| 800 | 295.262 | 182.929 | 303.375 |

*NLO properties*

Nonlinear optics properties of metal complexes have been the subject of extensive investigations during recent decades because of its potential in optical electronic application such as electro-optical (EO) switches [40,41] Zhang and coworkers showed that [HL] is a good candidate for NLO material [15]. For investigation of NLO properties of [CuL(phen)], it was screened for this compound by the quasi-Kurtz powder technique. A comparison of the area of second harmonic generation (SHG) signal emitted by the

**Table 8**
The calculated electric dipole moments (Debye), static polarizability components (a.u.), first hyperpolarizability components (a.u.) of [HL] and [CuL(phen)].

| Parameters | [HL] | [CuL(phen)] |
|---|---|---|
| $\mu_x$ | −1.024 | 3.278 |
| $\mu_y$ | −0.477 | −0.926 |
| $\mu_z$ | 0 | 0.423 |
| $\alpha_{xx}$ | 223.280 | 354.131 |
| $\alpha_{yy}$ | 117.528 | 272.042 |
| $\alpha_{zz}$ | 46.585 | 271.984 |
| $\beta_{xxx}$ | −155.196 | −60.982 |
| $\beta_{xxy}$ | 11.240 | −202.661 |
| $\beta_{xyy}$ | −12.409 | −74.544 |
| $\beta_{yyy}$ | −108.716 | −227.067 |
| $\beta_{xxz}$ | 1.736 | 95.474 |
| $\beta_{yyz}$ | −2.018 | 14.908 |
| $\beta_{xzz}$ | −18.845 | 47.698 |
| $\beta_{yzz}$ | 16.905 | 24.320 |
| $\beta_{zzz}$ | −0.274 | −140.129 |

**Table 9**
Selected Wiberg bond index (WBI) of title complex.

| Wiberg | Bond index | Wiberg | Bond index | Wiberg | Bond index |
|---|---|---|---|---|---|
| $W_{Cu-N1}$ | 0.2339 | $W_{C20-O2}$ | 1.2731 | $W_{C15-C14}$ | 1.5080 |
| $W_{Cu-N2}$ | 0.1598 | $W_{C20-N4}$ | 1.5168 | $W_{C14-C13}$ | 1.2868 |
| $W_{Cu-N3}$ | 0.3552 | $W_{N3-C19}$ | 1.5852 | $W_{C13-O1}$ | 1.2205 |
| $W_{Cu-O1}$ | 0.3967 | $W_{C19-C18}$ | 1.1845 | $W_{N2-C10}$ | 1.4730 |
| $W_{Cu-O2}$ | 0.3494 | $W_{C18-C17}$ | 1.3211 | $W_{N2-C11}$ | 1.3074 |
| $W_{C21-C20}$ | 1.0097 | $W_{C17-C16}$ | 1.4954 | $W_{C18-C13}$ | 1.2200 |
| $W_{N4-N3}$ | 1.0917 | $W_{C16-C15}$ | 1.3495 | $W_{C5-C6}$ | 1.6461 |
| $W_{C12-N1}$ | 1.2871 | $W_{C2-C3}$ | 1.5118 | $W_{C9-C10}$ | 1.3401 |
| $W_{C1-N1}$ | 1.4455 | $W_{C3-C4}$ | 1.3064 | $W_{C8-C9}$ | 1.5180 |
| $W_{C1-C2}$ | 1.3487 | $W_{C4-C5}$ | 1.2784 | $W_{C7-C8}$ | 1.3039 |
| $W_{C7-C11}$ | 1.2761 | $W_{C11-C12}$ | 1.1416 | | |

**Table 10**
In vitro antimicrobial activity of the compounds, 5000 μg/ml (IZ).

| Microorganism | [HL] dia. of clear zone (mm) | [CuL(phen)] dia. of clear zone (mm) | Ciprofloxacin. dia. of clear zone (mm) | Fluconazol, dia. of clear zone (mm) |
|---|---|---|---|---|
| *E. coli* | 15 | 23 | 31 | 0 |
| *S. aureus* | 20 | 40 | 24 | 0 |
| *P. aeruginosa* | 8 | 11 | 19 | 0 |
| *L. monocytogenes* | 0 | 32 | 20 | 0 |
| *C. albicans* | 33 | 45 | 0 | 33 |

**Table 11**
In vitro antimicrobial activity of the compounds, (MIC, μg/ml).

| Compound | Microorganisms | | | | |
|---|---|---|---|---|---|
| | *E. coli* | *S. aureus* | *P. aeruginosa* | *L. monocytogenes* | *C. albicans* |
| [HL] | 225 | 125 | 625 | – | 62.5 |
| [CuL(phen)] | 78.0 | 62.5 | 125 | 62.5 | 39.0 |

sample with the standard urea under the same experimental conditions, showed that it is 1.4 times more than that for urea.

The calculated nonlinear optical parameters of title compounds are listed in Table 8. According to equations of [1–3], the calculated total static dipole moment ($\mu_0$) of [HL] and [CuL(phen)] complex are equal to 1.13 and 3.43 Debye respectively. The magnitude of mean polarizability ($\alpha_0$) of ligand and Cu(II) complex are 19.14 and 44.32 $Å^3$ respectivley and finally calculated values of first-order hyperpolarizability ($\beta_0$) were found to be 17.53 and 35.93 $cm^5$/esu, respectively for [HL] and [CuL(phen)] respectively

The higher values of these parameters and lower energy gap between HOMO and LUMO in case of [CuL(phen)] indicate the increase of NLO properties of Cu(II) complex in comparison with the free ligand.

*Wiberg bond index analysis*

Wiberg bond index (WBI) is a useful method for analyzing the type of bands in molecule. Selected bond index for [CuL(phen)] are listed in Table 9. According to it, all bonds between donor atoms and central atom in this complex have a covalent nature. In this case Cu—O bonds have larger bond order in compared with Cu—N. Also the interaction between the central metal and the N atom of the 1,10-phenanthroline moiety is remarkably weaker than that with the other atoms atoms, as proved by the wiberg bond indexes (WBI) less value of Cu—N bond order, causes the grater bond length the bond order of C20—N4 and C19—N3 are 1.5168 and 1.5852 respectively which is larger than 1.5 and is due to double bond attributed of them. All aromatic ring bonds order are smaller than 1.5 which indicates the presence of $p$–$\pi$ conjugation among contributed atoms.

*Antimicrobial activity*

The antibacterial activity of [HL] and [CuL(phen)] ligands against *Escherichia coli, Staphylococcus aureus, Pseudomonas aeruginosa, Listeria monocytogenes* and *Candida albicans* was assessed by evaluating the presence of inhibition zone (IZ) and MIC values. Results (Table 10), showed that the [HL] and [CuL(phen)] have great potential of antibacterial and antifungal activity. It seems that the antibacterial effect of [HL] is not more on Gram negative bacteria. However, [CuL(phen)] are very effective both Gram negative and Gram positive bacteria. The MIC values for the ligands were in the range of 4.9–5000 μg/ml. The results of our study showed that the ligands were effective on bacteria and *C. albicans* (Table 11). According to the results we found that the [HL] and [CuL(phen)] have antibacterial and antifungal activity. The more activity of complex against bacteria and fungus is due to the positive charge of central atom shared with donor atoms of [HL] and $\pi$-electron delocalization in over the whole chelate moiety hence the lipophilic nature of complex will be increased so this makes it stronger in penetrating through the lipid layers of microbial membranes, that means it will be a better anti-microbial agent.

## Conclusions

The tridentate ONO Schiff base ligand (*E*)-*N′*-(2-hydroxybenzylidene) acetohydrazide [HL] and its mixed ligand Cu(II) complex were synthesized and characterized by spectroscopic methods such as FT-IR, CHN and UV–Vis. X-ray diffraction was also performed on Cu(II) complex. From spectral characterization, it was included that the metal complex has square pyramidal geometry. DFT calculations were performed to predict the structural geometry and interpret the NLO properties as well as experimental data. The higher first hyper-polarizability ($\beta$), polarizability ($\alpha$) and dipole moment ($\mu$) as well as the lower HOMO–LUMO gap of the [CuL(phen)] compared to the [HL], indicate the high NLO properties of the Cu(II) complex. The SHG efficiency of the complex was measured by the Kurtz-powder technique, and the results indicate that [CuL(phen)] possesses promising potential for the application as useful NLO material. In addition, experimental investigation shows that these compounds have antibacterial activity against *E. coli, S. aureus, P. aeruginosa,* and *L. monocytogenes.* They act as antifungal agents against *C. albicans* Results showed that [CuL(phen)] has a stronger antibacterial effect against all bacterial varieties in comparison with [HL] Schiff base ligand.

## Acknowledgements

Authors gratefully acknowledge the financial support provided for this work by the Shahid Bahonar University of Kerman as well the University of Fribourg. We thank optic laboratory in valie asr University (Rafsanjan) for the provision of Nd:YAG laser.

## Appendix A. Supplementary material

Supplementary data associated with this article can be found, in the online version

## References


[1] (a) M. Maiti, D. Sadhukhan, S. Thakurta, S. Sen, E. Zangrando, R.J. Butcher, R.C. Deka, S. Mitra, Eur. J. Inorg. Chem. 2013 (2013) 527–536;
(b) O.M.I. Adly, A. Taha, S.A. Fahmy, J. Mol. Struct. 1054 (2014) 239–250.
[2] M. Choudhary, R.N. Patel, S.P. Rawat, J. Mol. Struct. 1060 (2014) 197–207.
[3] S. Biswas, A. Dutta, M. Debnath, M. Dolai, K.K. Das, M. Ali, Dalton Trans. 42 (2013) 13210–13219.
[4] Y. Niu, Z. Li, Y. Song, M. Tang, B. Wu, X. Xin, J. Solid State Chem. 179 (2006) 4003–4010.
[5] K.J. Waldron, J.C. Rutherford, D. Ford, N.J. Robinson, Nature 460 (2009) 823–830.
[6] Y. Lu, N. Yeung, N. Sieracki, N.M. Marshall, Nature 460 (2009) 855–862.
[7] A.L. Abuhijleh, J. Khalaf, Eur. J. Med. Chem. 45 (2010) 3811–3817.
[8] T. Fukai, M. Ushio-Fukai, Antioxid. Redox signal. 15 (2011) 1583–1606.
[9] J. Perry, D. Shin, E. Getzoff, J. Tainer, BBA-Proteins Proteom. 1804 (2010) 245–262.
[10] S.A. Poteet, M.B. Majewski, Z.S. Breitbach, C.A. Griffith, S. Singh, D.W. Armstrong, M.O. Wolf, F.M. MacDonnell, J. Am. Chem. Soc. 135 (2013) 2419–2422.
[11] S. Anbu, A. Killivalavan, E.C.B.A. Alegria, G. Mathan, M. Kandaswamy, J. Coord. Chem. 66 (2013) 3989–4003.
[12] B.E. Halcrow, W.O. Kermack, J. Chem. Soc. (Resumed) (1946) 155–157.
[13] N.M. Urquiza, M. Soledad Islas, M.L. Dittler, M.A. Moyano, S.G. Manca, L. Lezama, T. Rojo, J.J. Martínez Medina, M. Diez, L. López Tévez, P.A.M. Williams, E.G. Ferrer, Inorg. Chim. Acta 405 (2013) 243–251.
[14] (a) S.S. Chavan, V.A. Sawant, A.N. Jadhav, Spectrochim. Acta A 117 (2014) 360–365;
(b) S.T. Chew, K.M. Lo, S.K. Lee, M.P. Heng, W.Y. Teoh, K.S. Sim, K.W. Tan, Eur. J. Med. Chem. 76 (2014) 397–407;
(c) L.S. Kumar, K.S. Prasad, H.D. Revanasiddappa, Eur. J. Chem 2 (3) (2011) 394–403.
[15] R. Takjoo, J.T. Mague, A. Akbari, S.Y. Ebrahimipour, J. Coord. Chem. 66 (2013) 2852–2862.
[16] H. Zhang, Y. Sun, X. Chen, X. Yan, B. Sun, J. Cryst. Growth 324 (2011) 196–200.
[17] A.D. Becke, J. Chem. Phys. 98 (1993) 5648–5652.
[18] C. Lee, W. Yang, R.G. Parr, Phys. Rev. B 37 (1988) 785–789.
[19] M.J. Frisch, G.W. Trucks, H.B. Schlegel, G.E. Scuseria, M.A. Robb, J.R. Cheeseman, J.A. Montgomery, T. Vreven, K.N. Kudin, J.C. Burant, J.M. Millam, S.S. Iyengar, J. Tomasi, V. Barone, B. Mennucci, M. Cossi, G. Scalmani, N. Rega, G.A. Petersson, H. Nakatsuji, M. Hada, M. Ehara, K. Toyota, R. Fukuda, J. Hasegawa, M. Ishida, T. Nakajima, Y. Honda, O. Kitao, H. Nakai, M. Klene, X. Li, J.E. Knox, H.P. Hratchian, J.B. Cross, V. Bakken, C. Adamo, J. Jaramillo, R. Gomperts, R.E. Stratmann, O. Yazyev, A.J. Austin, R. Cammi, C. Pomelli, J.W. Ochterski, P.Y. Ayala, K. Morokuma, G.A. Voth, P. Salvador, J.J. Dannenberg, V.G. Zakrzewski, S. Dapprich, A.D. Daniels, M.C. Strain, O. Farkas, D.K. Malick, A.D. Rabuck, K. Raghavachari, J.B. Foresman, J.V. Ortiz, Q. Cui, A.G. Baboul, S. Clifford, J. Cioslowski, B.B. Stefanov, G. Liu, A. Liashenko, P. Piskorz, I. Komaromi, R.L. Martin, D.J. Fox, T. Keith, A. Laham, C.Y. Peng, A. Nanayakkara, M. Challacombe, P.M.W. Gill, B. Johnson, W. Chen, M.W. Wong, C. Gonzalez, J.A. Pople, Gaussian 03, Revision C.02, 2003.
[20] J.P. Perdew, K.A. Jackson, M.R. Pederson, D.J. Singh, C. Fiolhais, Phys. Rev. B 46 (1992) 6671–6687.
[21] A.E. Reed, L.A. Curtiss, F. Weinhold, Chem. Rev. 88 (1988) 899–926.
[22] N.M. O'Boyle, A.L. Tenderholt, K.M. Langner, J. Comput. Chem. 29 (2008) 839–845.
[23] E. Blanc, D. Schwarzenbach, H.D. Flack, J. Appl. Crystallogr. 24 (1991) 1035–1041.
[24] G.M. Sheldrick, SHELX-97: program for crystal structure refinement, University of Göttinge, 1997.
[25] S. Irshad, M. Mahmood, F. Perveen, Res J. Bio. 2 (2012) 1–8.
[26] CLSI, Methods for Dilution Antimicrobial Susceptibility Tests for Bacteria That Grow Aerobically, Approved Standard, M07-A9, Wayne, PA, USA, 2012.
[27] A. Cinarli, D. Gürbüz, A. Tavman, A.S. Birteksöz, Chin. J. Chem. 30 (2012) 449–459.
[28] A.W. Addison, T.N. Rao, J. Reedijk, J. van Rijn, G.C. Verschoor, J. Chem. Soc., Dalton Trans. (1984) 1349–1356.
[29] U.L. Kala, S. Suma, M.R.P. Kurup, S. Krishnan, R.P. John, Polyhedron 26 (2007) 1427–1435.
[30] P.B. Sreeja, M.R. Prathapachandra Kurup, A. Kishore, C. Jasmin, Polyhedron 23 (2004) 575–581.
[31] H.Y. Wang, Y.-H. Shi, H.-Y. Liu, J. Coord. Chem. 65 (2012) 2811–2819.
[32] S. Mazurek, A. Mucciolo, B.M. Humbel, C. Nawrath, Plant J. 74 (2013) 880–891.
[33] I. Sheikhshoaie, S.Y. Ebrahimipour, A. Crochet, K. Fromm, Res. Chem. Intermed. (2013) 1–11.
[34] S.Y. Ebrahimipour, J.T. Mague, A. Akbari, R. Takjoo, J. Mol. Struct. 1028 (2012) 148–155.
[35] I. Sheikhshoaie, S.Y. Ebrahimipour, M. Sheikhshoaie, H.A. Rudbari, M. Khaleghi, G. Bruno, Spectrochim. Acta A 124 (2014) 548–555.
[36] V. Balachandran, G. Santhi, V. Karpagam, A. Lakshmi, Spectrochim. Acta A 110 (2013) 130–140.
[37] O. Diouf, D.G. Sall, M.L. Gaye, A.S. Sall, C. R. Chimie 10 (2007) 473–481.
[38] V. Philip, V. Suni, M.R. Prathapachandra Kurup, M. Nethaji, Polyhedron 25 (2006) 1931–1938.
[39] K.M. Vyas, R.N. Jadeja, D. Patel, R.V. Devkar, V.K. Gupta, Polyhedron 65 (2013) 262–274.
[40] D.R. Kanis, M.A. Ratner, T.J. Marks, Chem. Rev. 94 (1994) 195–242.
[41] S.R. Marder, J.W. Perry, Adv. Mater. 5 (1993) 804–815.